How to mathematically evaluate whether a rigid flat-foldable origami design will unravel or not, and whether it will unravel completely or incompletely when pulled from two points?

Extended Essay in Mathematics Analysis and Approaches

Toma Kamata Sydnes

Contents

1 Introduction

Origami is an ancient Japanese art, involving the folding of uncut paper into structures through geometric manipulations (Meloni et al. 2021). Today origami has gone beyond paper and art finding applications in fields from aerospace to nanorobotics (ibid.). Origami principles also help explain biomechanical systems, from leaves (Dureisseix 2012) to microorganisms (Flaum and Prakash 2024). The usefulness of origami comes from its compact deployable system applying to both 2D and 3D structures; its transfer of mechanical force; and its self-actuation properties, which are all scale-free (Meloni et al. 2021). However, one must understand the underlying mathematical properties and restrictions to use origami to its fullest. Several mathematicians have found interest in this branch of geometry, discovering underlying axioms and theorems (Hull 2021); developing origami designing algorithms (Lang 1996; Lang 2011); and folding simulators (Mitani 2012; Tachi 2009). However, origami mathematics is still young and there are many unanswered questions. One such question is what the criteria for origami unraveling are. Why do some designs unravel when pulled and others do not? No literature was found to have explored this question, hence it was developed into the Extended Essay research question "How to mathematically evaluate whether a rigid flat-foldable origami design will unravel or not, and whether it will unravel completely or incompletely when pulled from two points?", which is defined in the Preliminary section. This question will be explored through experimentation to find patterns; geometric analysis to explain and understand observations; and development of theorems. Finding an answer to this question will provide an algorithm to theoretically analyze origami unravelability (the extent to which an origami design can unravel), reducing the need for experimental testing.

2 Preliminary

To explore this research question some preliminary definitions and clarifications must be made. Firstly origami must be defined (Definition 1 and 2).

Definition 1. *Origami is strictly defined as structures folded from a flat sheet* ($\mathbb{R}^2$) *(Hull 2021) where any two points* (A, B) *on the sheet have a straight-line segment* ($\overline{\mathrm{AB}}$) *on the sheet (Expression 1).*

$$\overline{\mathrm{AB}} \subset \mathbb{R}^2 \tag{1}$$

Definition 1 was inspired by Talagrand's lecture on his Abel prize-winning work at University of Stavanger (Talagrand 2024).

Definition 2. *Origami structures are folded from a non-cut sheet where no two faces,* s_a *and* s_b*, intersect* ($s_a \cap s_b$) *(Hull 2021).*

Both Definition 1 and 2 are common definitions in origami literature (ibid.), but in this Extended Essay, origami is further restricted to rigid origami (Definition 3).

Definition 3. *Rigid origami is any origami (Definition 1) where the sheet is only permitted to deform along crease lines (Misseroni et al. 2024).*

Definition 3 is a common restriction in origami application research, as it is the condition of most mechanical systems (Hull 2021; Meloni et al. 2021;

Misseroni et al. 2024). All three definitions (Definition 1, 2, and 3) permit origami to extend beyond the traditional restrictions, allowing origami to be structures folded from rigid sheets of any material, ranging from steel to polymer composites (Deleo et al. 2020), increasing applicability to the various mechanical fields(Meloni et al. 2021).

When researching origami a common approach is to investigate crease patterns (Figure 1) (Hull 2021). A crease pattern is a diagram representing folds as lines on a plane (Eppstein 2018), distinct to the specific folded structure (Hull 2021) and can therefore be used as a folding guide (Lang 2011). Each crease pattern is defined by its creases, vertices, and faces (Meloni et al. 2021). Faces are the blank areas surrounded by crease lines or the edge of the sheet. Looking at Figure 1 one quickly notices that all crease lines are

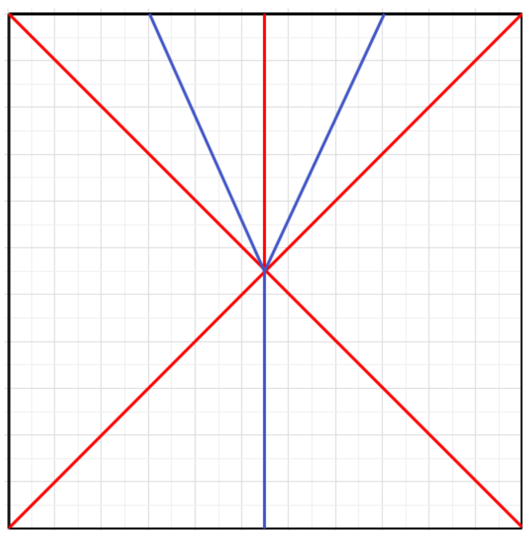

Figure 1: Single-vertex flat foldable crease pattern

straight. This is because this Extended Essay will only consider axiomatic origami, origami designs with crease patterns following Huzita-Hatori axioms (Ben-Ari 2022), also known as Basic Origami Operations (Hull 2021). This constraint aligns with the research question's focus on rigid, flat-foldable origami, which are all axiomatic. The choice to limit the scope to axiomatic designs is intentional, as they have a well-defined mathematical framework based on Euclidean geometry. In contrast, non-axiomatic designs lack formal geometric rules, therefore it would introduce complexities and ambiguities to the research. Huzita-Hatori axioms are briefly presented in Figure 2, but understanding them is not required for this essay. However, note that the operations can only produce straight creases.

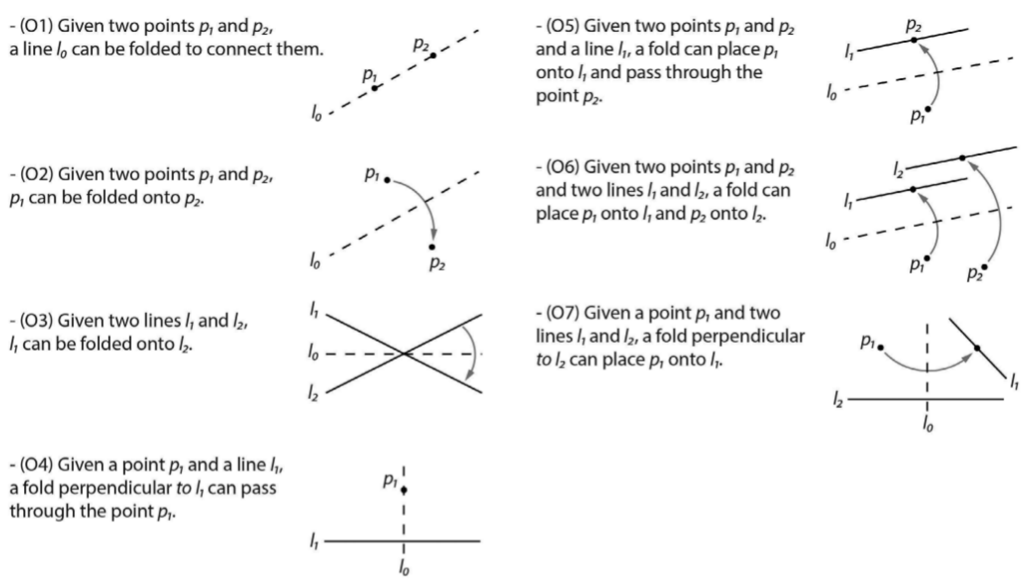

Figure 2: Brief presentation of Huzita-Hatori axioms (Meloni et al. 2021)

When drawing these straight lines it is common practice to identify the fold type; whether it is a mountain or a valley fold. In this essay, red lines represent mountain folds while blue lines represent valley folds. Both mountain and valley folds are visualized in Figure 3 and defined in Definition 4 and 5.

Definition 4. *Valley folds are folds with fold angle θ where $0 < \theta \leqslant \pi$ (Meloni et al. 2021)*

Definition 5. *Mountain folds are folds with fold angle θ where $-\pi \leqslant \theta < 0$ (ibid.)*

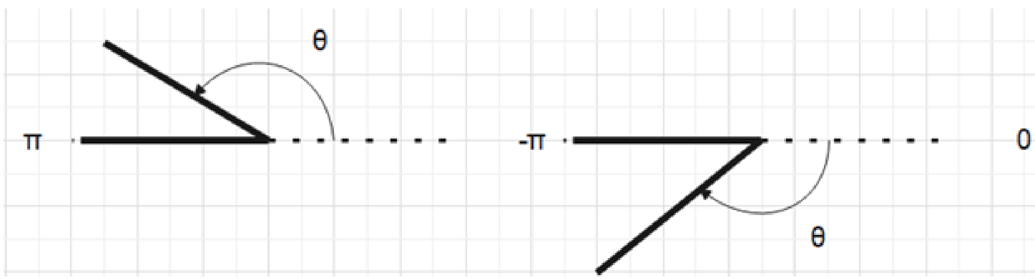

Figure 3: Left: valley fold, Right: mountain fold, inspired by Hull (2021)

Further, the research question is restricted to flat-foldable origami, a subsection where all origami must fold flat (Hull 2021). For this, it must follow Definition 6.

Definition 6. *For a crease pattern to be flat-foldable each crease must have a folding angle that converges to either π or $-\pi$ (ibid.).*

One such example is the crease pattern in Figure 1. Whether the crease pattern is flat-foldable can be tested experimentally by folding (Figure 4) or checked theoretically using Maekawa's theorem and Kawasaki's theorem (ibid.).

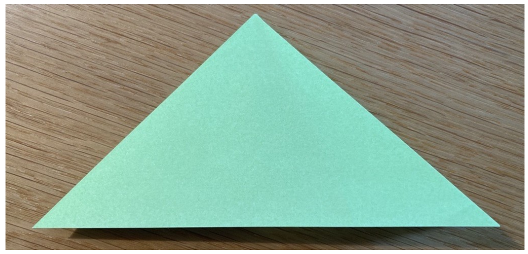

Figure 4: Figure 1 crease pattern folded confirming its flat-foldability

Theorem 1 (Maekawa's theorem)**.** *"The difference between the number of mountain (M) and valley (V) creases in a flat vertex fold on a cone with cone angle $\leqslant 2\pi$ is 2" (Expression 2) (Hull 2021).*

$$|M - V| = 2 \tag{2}$$

Theorem 2 (Kawasaki's theorem)**.** *"Let G be a single-vertex crease pattern on a cone with cone angle $\leqslant 2\pi$ and with consecutive angles between the creases $\alpha_0, ..., \alpha_{2n-1}$. Then G is flat-foldable if and only if $\alpha_0 - \alpha_1 + \alpha_2 - ... - \alpha_{2n-1} = 0$" (ibid.).*

The research question is limited to flat-foldable origami designs to reduce the ambiguity of "unraveling". According to Defintion 6 a flat-foldable origami design when folded must have fold angles π or $-\pi$, hence a flat-foldable crease has only two states, folded ($|\theta| = \pi$) or unraveled ($\theta = 0$) (Definition 7). This is useful when operationalizing the states of unraveling: not unraveled (Definition 8), incompletely unraveled (Definition 9), and completely unraveled (Definition 10).

Definition 7. *A flat-foldable crease is folded when its fold angle* $\theta = \pi$ *or* $-\pi$ *and unraveled when its fold angle* $\theta = 0$.

Definition 8. *An origami structure is not unraveled when all* n *creases are folded (Definition 7). Hence, a flat-foldable origami (Definition 6) is not unraveled iff* $\sum_{k=1}^{n} |\theta_k| = \pi n$.

Definition 9. *An origami structure is incompletely unraveled when* p *(*$0 < p < n$*) creases are unraveled (Definition 7) and when* $n - p$ *creases are folded (Definition 7). Hence, a flat-foldable origami (Definition 6) is incompletely unraveled iff* $0 < \sum_{k=1}^{n} |\theta_k| < \pi n$.

Definition 10. *An origami structure is completely unraveled when all* n *creases have unraveled (Definition 7). Hence, a flat-foldable origami (Definition 6) is completely unraveled iff* $\sum_{k=1}^{n} |\theta_k| = 0$.

According to Definition 7 and 10, when a crease unravels or when an entire crease pattern unravels completely it should turn flat returning to the condition before folding. However, when experimenting with paper the deformations' of the creases are permanent preventing the paper from turning completely flat. Hence, paper is not an ideal medium to simulate the mathematical ideal, limiting the validity of observations. Regardless it still serves a valuable purpose in aiding the imagination of the ideal and the theoretical analysis. Therefore experimentation will remain essential in the exploration of the research question but the results must be critically evaluated.

Finally, pulling is defined in Definition 11. With this all elements of the research question is defined providing clear boundaries and a rigid framework to start mathematical exploration.

Definition 11. *Pull is defined to act from two non-overlapping points, P_1, P_2, on the sheet ($\mathbb{R}^2$) (Expression 3) with vectors in opposing permanent directions.*

$$P_1 \neq P_2 \land P_1, P_2 \cap \mathbb{R}^2 \neq \varnothing \tag{3}$$

3 Investigating single-vertex origami

To solve the research question the simplest origami design had to be investigated at first. The simplest origami designs are single-vertex designs, where the crease pattern only has one vertex from which straight creases radiate to the edge of the sheet (Figure 1) (Hull 2021). Since Figure 1 is a single-vertex design, this section will use the crease pattern in Figure 1 to explain results of the exploration.

Firstly, to systematically explore the effect of differing points of pull, the pulling points were first restricted to be on the creases, which were numbered in a clockwise manner (Figure 5). Allowing systematic experimentation of unraveling when pulling from different combinations of points. Results for Figure 1 are tabulated in Table 1. Here, the creases that unraveled when pulling from C_1 and a different crease are summarized, denoted using the crease numbering in Figure 5. The pulling points' (P_1, P_2) (Definition 11) positions on the creases are not noted as they did not affect the unravelability. Therefore, all the following visualizations of the pull are represented using green arrows starting from the edge of the crease, allowing for a clearer visualization (Figure 6). However, it should be mentioned that the position affected the force required to unravel, but this is ignored as it is irrelevant to answer the research question.

Based on the data collected (Table 1), when two neighboring creases are pulled nothing unravels. Therefore, when Expression 4 is true, there is no

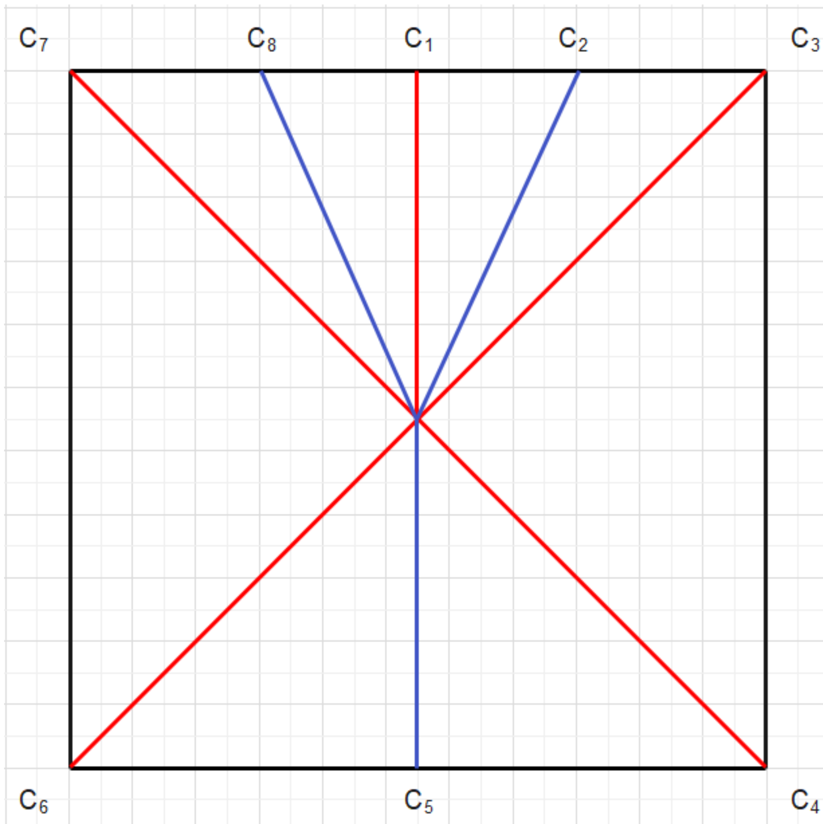

Figure 5: Figure 1 with creases numbered in a clockwise order

Creases with point of pull	Creases unraveled
C_1, C_2	none
C_1, C_3	C_2
C_1, C_4	C_2, C_3
C_1, C_5	$C_2, C_3, C_4, C_6, C_7, C_8$
C_1, C_6	C_7, C_8
C_1, C_7	C_8
C_1, C_8	none

Table 1: Tabulation of the position of points of pull and which creases unraveled.

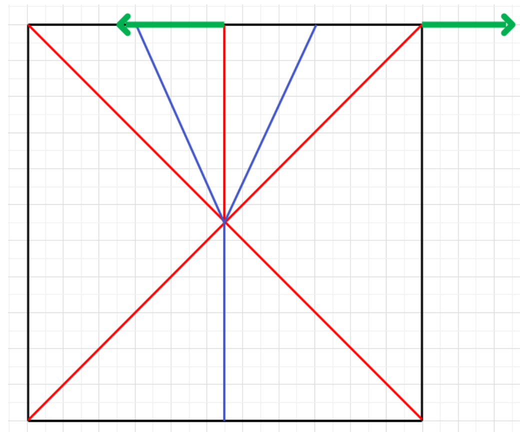

Figure 6: Visualization of pull

unraveling. Finding the criterion for no unraveling, answering a part of the research question.

$$\begin{aligned} P_1 \in & C_x \wedge P_2 \in \{C_{x+1},\ C_{x-1}\},\ x \in \mathbb{Z}^+,\ x \leqslant n \\ & \text{if } x = n,\ C_{x+1} = C_1, \text{ if } x = 1,\ C_{x-1} = C_n \end{aligned} \tag{4}$$

3.1 Line of tension and crease unraveling

There is also a pattern for creases unraveled which is best understood by drawing a straight line between the two pulling points (P_1, P_2) (Definition 11). From Table 1 it is evident that all the creases intersecting this line $(\overline{P_1P_2})$ unravel, except the two creases with the pull points (P_1, P_2). These patterns were observed in all trials and are best explained by understanding the line $(\overline{P_1P_2})$ as a line of tension T. The interpretation of the line of tension is justified by tension's tendency to follow the shortest path between two points, when forces act in opposite directions (Definition 11), and by Definition 3, prohibiting deformation of the sheet, satisfying the criteria for tension formation.

To further understand this interpretation one should start by investigating an individual fold (Figure 7; red line). The effect of the line of tension (T) can be understood by treating T as two vectors ($\vec{T_1}$, $\vec{T_2}$) extending from the intersection between T and the crease (Figure 7; black solid line). Each of the two pulling vectors can be decomposed into a vector parallel ($\vec{T_y}$) and normal ($\vec{T_x}$) to the crease (Figure 7; black dotted lines). The parallel vectors

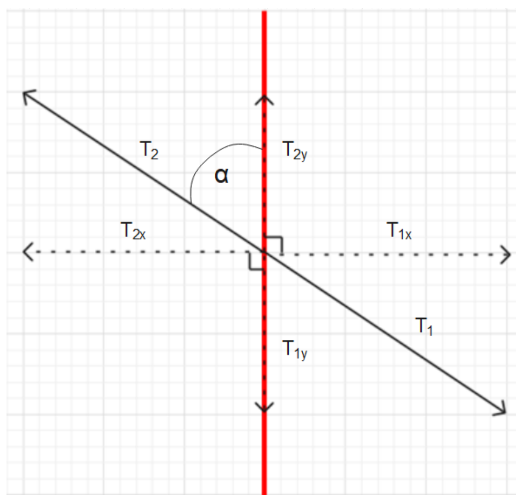

Figure 7: Decomposition of vector T over a crease (red)

are ignored as they cannot change the system, as origami is defined on a non-stretchable sheet (Definition 3). However, the normal vectors will unravel the fold (Figure 8). Therefore, there are two conditions for a crease to unravel developed into Theorem 3

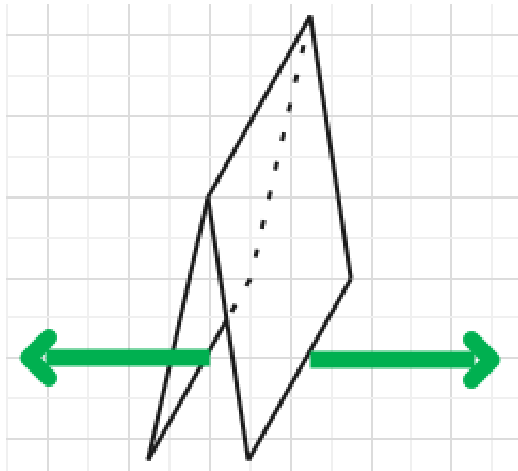

Figure 8: Unfolding of a 3-dimensional diagram of Figure 7

Theorem 3. *Given a single-vertex rigid flat foldable origami, any crease C_k unravels when the line of tension T intersects C_k at only one point.*

Proof. Assume the contrary is true, that the crease C_k unravels when intersecting T at two or more points.

Since only axiomatic origmai are considered, the geometry must adhere to Euclidean principles. In Euclidean geometry, when two straight lines intersect at two or more points the two lines are coincident.

T_x can be rewritten in terms of T and α, where α is the angle between the line of tension (T) and the crease (C_k) (Expression 5) (Figure 7).

$$T_x = T \sin \alpha \tag{5}$$

When T and C_k are coincident $\alpha = 0$, hence, by solving Expression 5 for

$\alpha = 0$ one can find the value of T_x.

$$T_x = T \sin 0$$

$$T_x = 0$$

If $T_x = 0$ there is no unraveling. Hence, it is proven that C_k does not unravel when T intersects C_k at more than one point. QED

Whether a crease unravels can therefore be checked mathematically using Expression 6, a mathematical formulation of Theorem 3. When Expression 6 is true the crease (C_k) unravels. G_T is the gradient of T and G_{C_k} is the gradient of C_k, and are used to check whether T and C_k are coincident (parallel). Therefore, this logic answers the research question for a singular crease, but it must be extended to cover an entire design.

$$G_T \neq G_{C_k} \wedge T \cap C_k \neq \varnothing \tag{6}$$

An implication of the Theorem can be observed in Table 1. No combination of points of pull unravels all the creases. The one closest to completely unraveling the structure is pulling (Definition 11) from C_1 and C_5 (Table 1). When unraveling it unravels into a two-faced structure (Figure 9), as $G_T = G_{C_1}, G_{C_5}$ (Expression 6). Table 1 suggests a single-vertex origami will never completely unravel when points of pull lie on creases further detailed in Theorem 4.

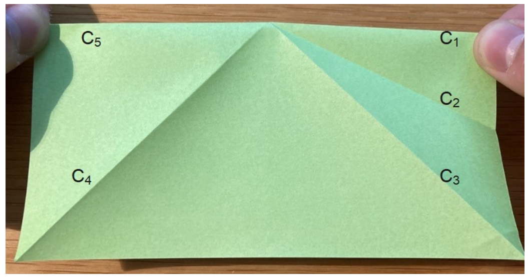

Figure 9: Resulting two-faced structure after pulling from C_1 and C_5 (turned horizontal)

Theorem 4. *Given a single-vertex rigid flat foldable origami, no two points, A, B, exist on creases, C_a, C_b $(a, b \in \mathbb{Z}^+,\ a \neq b,\ a, b \leqslant n)$, where two pulling forces (Definition 11) can completely unravel the entire structure.*

Proof. Assume the contrary is true, implying Expression 6 is true for pulling points A, B.

For this, T must intersect all the creases (Expression 6), only possible at the central vertex in a single-vertex-flat-foldable origami due to Kawasaki's theorem (Theorem 2). Therefore, the length of T must equal the added distance between A and the center (O) $(\overline{OA})$ and B and the center $(\overline{OB})$ (Expression 7).

$$T = \overline{OA} + \overline{OB} \tag{7}$$

Expression 7 can be rewritten in terms of coordinates by setting $O = (0, 0)$, $A = (x_a, y_a)$, and $B = (x_b, y_b)$ (Expression 8).

$$T = \sqrt{x_a^2 + y_a^2} + \sqrt{x_b^2 + y_b^2} \tag{8}$$

T can also be written using the cosine rule where φ is the intersection angle between $\overline{OA}$ and $\overline{OB}$(Expression 9).

$$T = \sqrt{\sqrt{x_a^2 + y_a^2}^2 + \sqrt{x_b^2 + y_b^2}^2 - 2\sqrt{x_a^2 + y_a^2}\sqrt{x_b^2 + y_b^2}\cos\varphi} \tag{9}$$

Combining both expressions gives Expression 10. Allowing one to find the angle φ where the assumption is true.

$$\begin{multline} \sqrt{x_a^2 + y_a^2} + \sqrt{x_b^2 + y_b^2} \\ = \sqrt{\sqrt{x_a^2 + y_a^2}^2 + \sqrt{x_b^2 + y_b^2}^2 - 2\sqrt{x_a^2 + y_a^2}\sqrt{x_b^2 + y_b^2}\cos\varphi} \end{multline} \tag{10}$$

$$\begin{multline} \left(\sqrt{x_a^2 + y_a^2} + \sqrt{x_b^2 + y_b^2}\right)^2 \\ = \sqrt{x_a^2 + y_a^2}^2 + \sqrt{x_b^2 + y_b^2}^2 - 2\sqrt{x_a^2 + y_a^2}\sqrt{x_b^2 + y_b^2}\cos\varphi \end{multline}$$

$$\begin{multline} x_a^2 + y_a^2 + x_b^2 + y_b^2 + 2\sqrt{x_a^2 + y_a^2}\sqrt{x_b^2 + y_b^2} \\ = x_a^2 + y_a^2 + x_b^2 + y_b^2 - 2\sqrt{x_a^2 + y_a^2}\sqrt{x_b^2 + y_b^2}\cos\varphi \end{multline}$$

$$2\sqrt{x_a^2 + y_a^2}\sqrt{x_b^2 + y_b^2} = -2\sqrt{x_a^2 + y_a^2}\sqrt{x_b^2 + y_b^2}\cos\varphi$$

$$1 = -\cos\varphi$$

$$-1 = \cos\varphi$$

$$\varphi = (2i + 1)\pi, i \in \mathbb{Z}$$

According to Maekawa's theorem and Kawasaki's theorem origami designs are only flat foldable if they are on a cone with a cone angle $\leqslant 2\pi$.

Hence $\varphi = -\pi, \pi$.

However when $\varphi = -\pi$ or π $G_{Ca}, G_{Cb} = G_T$, hence the design will not unravel (Theorem 3 and Expression 6),

Therefore, the assumption is false and the theorem is proven by contradiction.

QED

However, this impossibility is avoided when the pulling points (Definition 11) are not restricted to be points on crease lines (Figure 10). When Expression 6

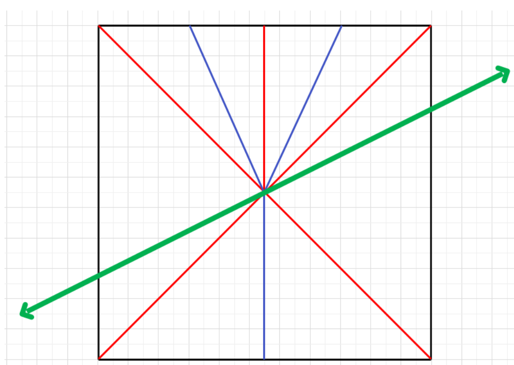

Figure 10: Figure 1 crease pattern with $T \cap C_{1\to n}$ and $G_T \neq G_{C_{1\to n}}$

is true the crease always unravels. Therefore whether a single-vertex origami design will unravel completely can be evaluated computationally using Expression 11, a loop checking whether Expression 6 is true for all creases from C_1 to C_n.

$$G_T \neq G_{C_{1\to n}} \wedge T \cap C_{1\to n} \neq \varnothing \tag{11}$$

With this additional logic, the research question is completely answered for single-vertex designs. Firstly, if Expression 11 is true the design completely unravels. Secondly, if Expression 11 is false and Expression 4 is false the design unravels incompletely. Thirdly, if $T \cap C_{1 \to n} \neq \varnothing$ is false or Expression 4 is true no unraveling.

4 Investigating multi-vertex origami

When testing the evaluation logic developed for single-vertex origami on multi-vertex origami the predictions are erroneous due to more complex unraveling motions and force distribution. Firstly, there are cases where the unraveling motions require an intersection between faces. Secondly, some designs have special force distributions, making creases unravel despite the line of tension T not intersecting the crease. The following sections will address these problems by exploring some specific multi-vertex origami designs. Solving this is essential to answer the research question as it includes single-vertex and multi-vertex origami.

4.1 Physical intersection of faces prohibiting unraveling

One of the simplest multi-vertex origami is the hand fan, consisting of parallel creases with alternating mountain and valley assignment (Figure 11).
When pulling from two ends of the sheet, as shown in Figure 12, the structure unravels as predicted by Expression 11, as T (Figure 12; green line) intersects all the creases at only one point each. However, when editing the design to have two consecutive mountain folds (Figure 13), the design unravels incompletely. This experimental result contradicts the logic developed for single-vertex designs (Expression 11). The expression's flaw is that it

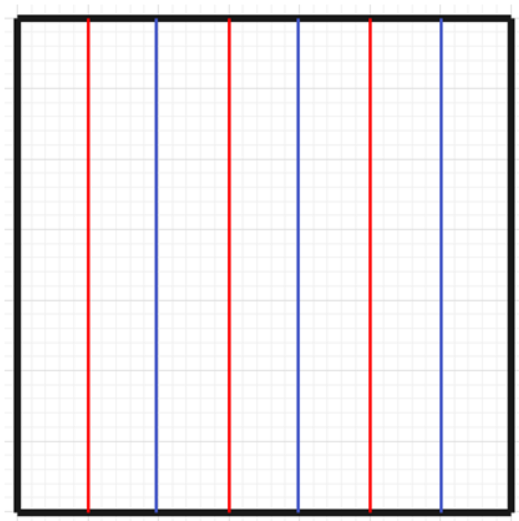

Figure 11: Origami hand fan crease pattern

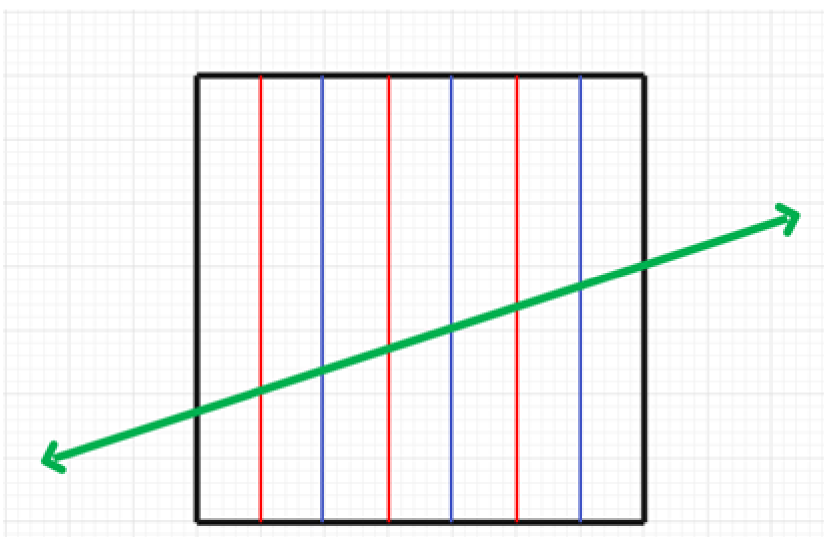

Figure 12: Origami hand fan where T intersects all creases and the design unravels

does not consider the fold type, whether mountain or valley. Therefore, this must be altered to produce an algorithm that can reliably predict whether a multi-vertex origami design will unravel.

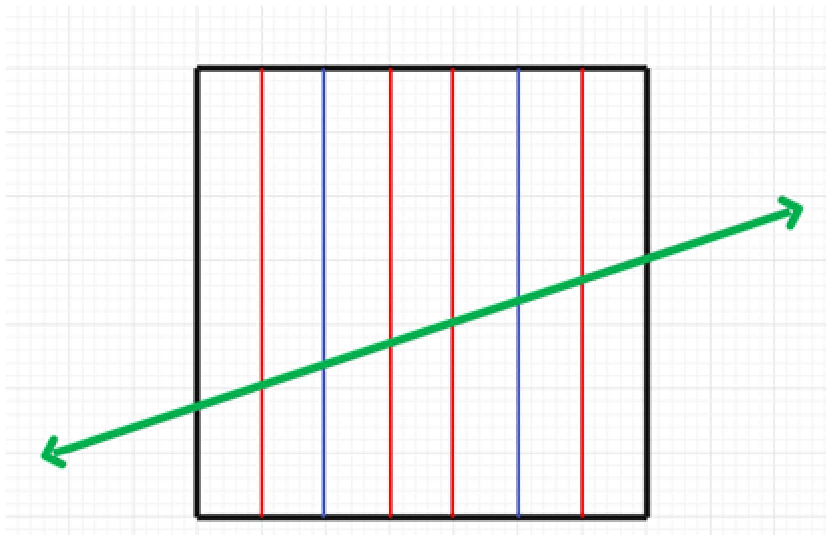

Figure 13: Origami hand fan with two consecutive mountain folds

To answer the research question the experimental results must first be understood, hence two explanations were proposed. The first explanation involves the formation of a curl (how the paper wraps around one of the pulling points). For the sheet to continue unraveling its faces would need to intersect and pass through one another, violating Definition 2. Although one may argue that rigid sheets (Definition 3) prohibit curling, a flexible sheet can be conceptualized as having infinite creases, allowing this theoretical interpretation. The second explanation focuses on the face orientations (which side is up), viewing folds as rotations around creases. If the pulling points are on faces with opposite orientations, the sheet curls because the faces cannot rotate due to the pull's permanent direction (Definition 11). This curling phenomenon occurs not only with consecutive mountain folds but also with consecutive valley folds.

To explore this phenomenon and potential explanations, mathematical simplifications are made. First, the dimensions of both the crease pattern and the folded structure are reduced (Expression 12 and 13), and the process is visualized in Figure 14 and 15, an approach inspired by Talagrand (2024). This is possible because the pulling vector only acts on the points of intersection between T and the creases. Hence the angle of intersection does not matter and a 2D crease pattern can be reduced into a 1D diagram of crease intersection points along T. By doing this diagrams become simpler and the mathematics easier to develop.

$$\mathbb{R}^2_{(creasepattern)} \to \mathbb{R}_{(creasepattern)} \tag{12}$$

$$\mathbb{R}^3_{(folding)} \to \mathbb{R}^2_{(folding)} \tag{13}$$

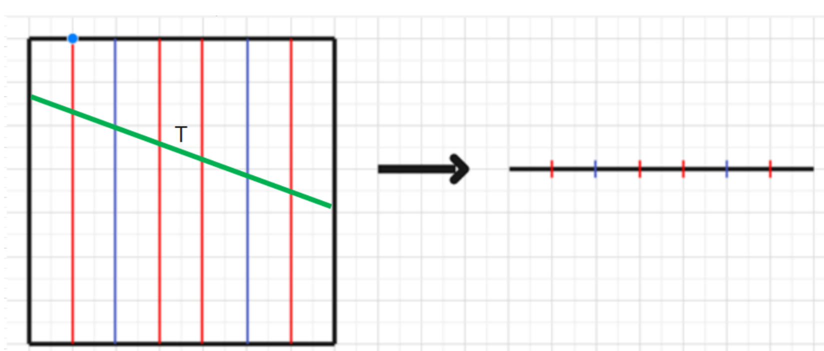

Figure 14: Visualization of Expression 12

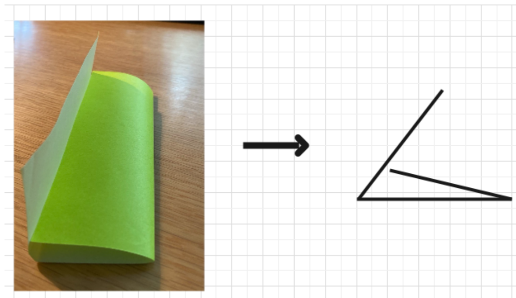

Figure 15: Visualization of Expression 13

Additionally, the experimentation method was simplified. Instead of having two pulling points (Definition 11) one can have a fixed point, and a pulling point, as this is equivalent to having two pulling points (Definition 11) when ignoring magnitude. This is permitted because the research question is not interested in the amount of force required to unravel, but rather in the geometric criteria for unraveling. Further, the simplification avoids accidental changes in the direction of the pulling vector, which is against Definition 11.

Based on the reductions (Expression 12 and 13), the folding process can be represented as done in Figure 16, where two valley creases produce three faces named s_1, s_2, and s_3. This is the simplest design with consecutive valley folds.

As illustrated in Figure 16 there are only two ways for this crease pattern to fold. Both combinations are better represented using matrices with one

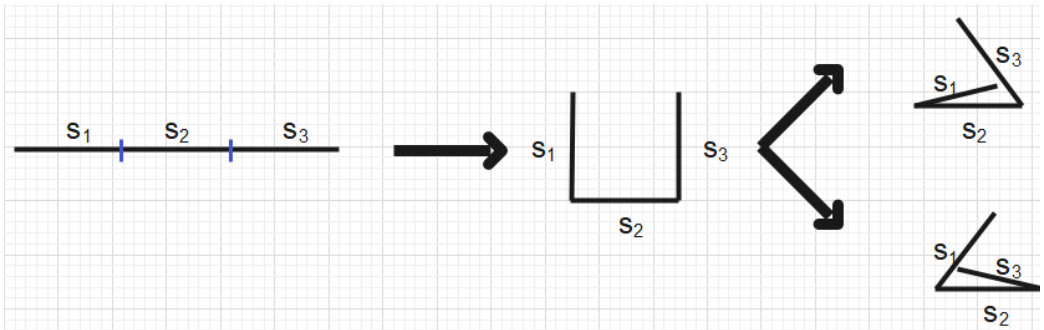

Figure 16: Folding sequence and possible folding orders of a two valley fold hand fan design

column (Expression 14).

$$\begin{bmatrix} s_3 \\ s_1 \\ s_2 \end{bmatrix} \qquad \begin{bmatrix} s_1 \\ s_3 \\ s_2 \end{bmatrix} \tag{14}$$

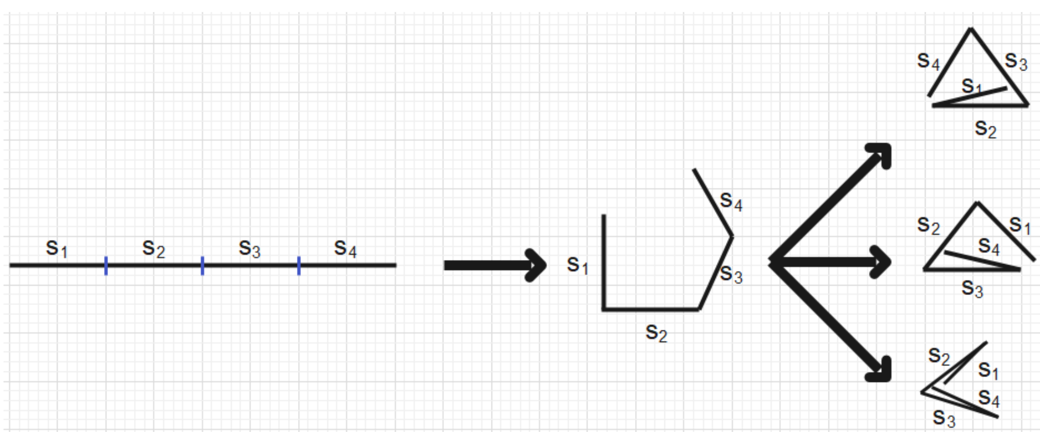

Figure 17: Folding sequence and possible folding orders of three valley fold hand fan design

When testing the unravelability of these hand fan arrangements (Figure

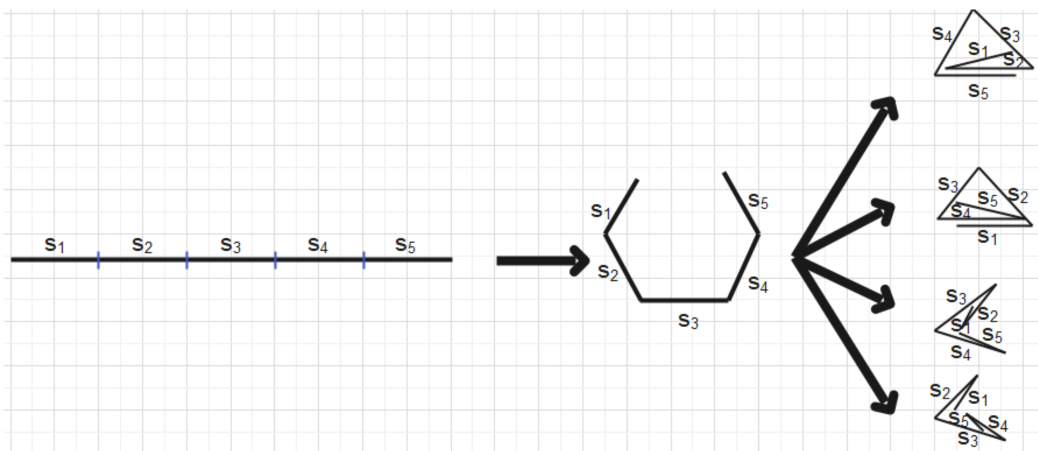

Figure 18: Folding sequence and possible folding orders of a four valley fold hand fan design

16, 17 and 18) a few patterns emerge. To better understand them the folded structure in Figure 17 and 18 are also represented as matrices in Expression 15 and 16.

$$\begin{bmatrix} s_3 \\ s_1 \\ s_2 \\ s_4 \end{bmatrix} \qquad \begin{bmatrix} s_2 \\ s_4 \\ s_3 \\ s_1 \end{bmatrix} \qquad \begin{bmatrix} s_2 \\ s_1 \\ s_4 \\ s_3 \end{bmatrix} \tag{15}$$

$$\begin{bmatrix} s_5 \\ s_3 \\ s_1 \\ s_2 \\ s_4 \end{bmatrix} \qquad \begin{bmatrix} s_1 \\ s_3 \\ s_5 \\ s_4 \\ s_2 \end{bmatrix} \qquad \begin{bmatrix} s_2 \\ s_1 \\ s_4 \\ s_5 \\ s_3 \end{bmatrix} \qquad \begin{bmatrix} s_4 \\ s_5 \\ s_2 \\ s_1 \\ s_3 \end{bmatrix} \tag{16}$$

There are several patterns (Expression 14, 15, and 16), but most importantly no matrix has both the first face, s_1, and the last face, $s_f(f = n+1)$, on the ends (top and bottom) (Expression 14, 15 and 16). This allows for one simple way to test whether a design will unravel completely by checking whether s_1 and s_f are each at the top and bottom of the matrix.

The inability of designs with only consecutive valley or mountain folds to unravel completely is proven (Theorem 5), important to provide certainty to the essay's answer to the research question.

Theorem 5. *No flat foldable rigid origami design with only m ($m = n$) consecutive valley or mountain folds ($m \geqslant 2, m \in \mathbb{Z}^+$) can unravel completely when pulled from two points (Definition 11).*

Theorem 5 can be reformulated into Lemma 1, which makes Theorem 5 easier to prove.

Lemma 1. *A design with only m number of consecutive valley or mountain folds cannot have s_1 on the top of a final folded structure whilst having s_f ($f > 2$, $f \in \mathbb{Z}^+$) at the bottom (Expression 17).*

$$\begin{bmatrix} s_1 \\ s_2 \\ \vdots \\ s_{f-1} \\ s_f \end{bmatrix} \tag{17}$$

Proof. Assume s_1 is at the top and s_f is at the bottom (Expression 17). Then s_2 must be below s_1 and s_{f-1} must be above s_f (Expression 17). This identity of above and below relative to the face before can be represented using a variable k ($1 \leqslant k < f$, $k \in \mathbb{Z}^+$). Where fold $s_1 \to s_2$ can be represented as fold $k = 1$, fold $s_2 \to s_3$ as $k = 2$, and fold $s_{f-1} \to s_f$ as $k = f - 1$. The results are tabulated in Table 2 showing a pattern between the above/below identity relative to the face before and k. When k is odd ($k = 2q - 1, q \in \mathbb{Z}^+$) $s_{2q-1} \to s_{2q}$ is below (s_{2q} is below s_{2q-1}) whilst when k is even ($k = 2q$) $s_{2q} \to s_{2q+1}$ is above (s_{2q+1} is above s_{2q}).

Fold	k value	above/below identity relative to the face
$s_1 \to s_2$	$k = 1$	below
$s_2 \to s_3$	$k = 2$	above
$s_3 \to s_4$	$k = 3$	below
$s_4 \to s_5$	$k = 4$	above
$s_5 \to s_6$	$k = 5$	below
$s_6 \to s_7$	$k = 6$	above

Table 2: Table of the vertical position relationship between flap sections

If s_f is at the bottom s_f must be below s_{f-1}, hence $k = f - 1$ is below.

If f is the odd number $2q-1$ the fold $s_{f-1} \to s_f$ can be rewritten as $s_{2(q-1)} \to s_{2q-1}$ which is above ($k = 2q-2 = 2(q-1)$) is even. However, this contradicts the assumption as s_f cannot be above s_{f-1} whilst being at the bottom of the folded structure.

Hence the assumption is false when f is odd.

When f is even, $f = 2q$, $f - 1$ is odd, $2q - 1$.

Hence s_{f-1} must be above s_{f-2} ($k = 2q - 2 = 2(q - 1)$).

When s_{f-1} is above s_{f-2}, s_f must either be between s_{f-1} and s_{f-2}, or above s_{f-1}, as the faces cannot intersect, pass through one another (Definition 2).
If s_f is above s_{f-1} the assumption is false as both s_{f-1} and s_{f-2} are below s_f.
If s_f is between s_{f-1} and s_{f-2} the assumption is false as s_{f-2} is below s_f.
Hence the assumption is also proven false when f is even.
Therefore the assumption is proven false for both even and odd f values, hence Theorem 5 is proven correct. QED

Further experimentation suggests that Theorem 5 also applies when the creases are not parallel. This is expected theoretically as T only acts on single points on the creases. Singular points can neither be parallel nor have an angle relative to one another, therefore it does not matter whether the creases are parallel or not. This is useful when answering the research question as it allows Theorem 5 to be extended beyond designs with parallel creases. On the other hand, experiments with designs with more than one group of consecutive valley or mountain creases (Figure 19) give differing results limiting Theorem 5 to one colony designs. A colony is a group of consecutive valleys or mountain creases, for example, Figure 19 is a two-colony design. However, to answer the research question the criteria for unraveling in multi-colony designs are also uncovered.

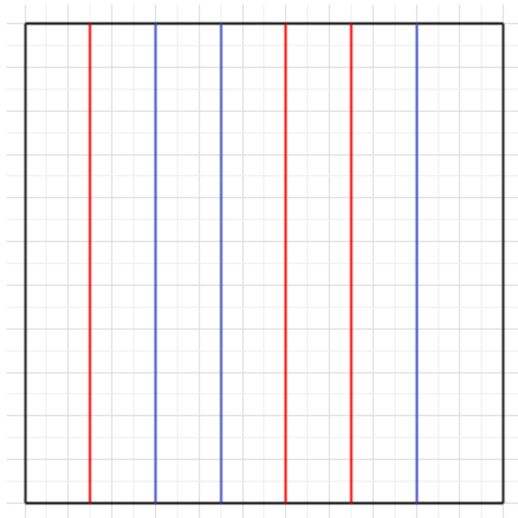

Figure 19: Multi colony origami

4.1.1 Multi colony designs

When attempting to explain the unraveling of a multi-colony design one cannot use the approach used for Theorem 5, as s_1 and s_f can be on top, at the bottom, in the middle, and on each end, because more freedom is granted. Therefore the second interpretation presented at the start of Section 4.1 will be used.

In this case, the difference in orientation between s_1 and s_f (whether the two faces have the same side up) is important. Each valley fold rotates faces by π radians (Definition 4 and 6), while every mountain fold can undo the rotation as it rotates faces by $-\pi$ radians (Definition 5 and 6). Since T must intersect all creases (Expression 11) one can use the difference in the total number of mountain creases (M) and valley creases (V) to find the total rotation (β)

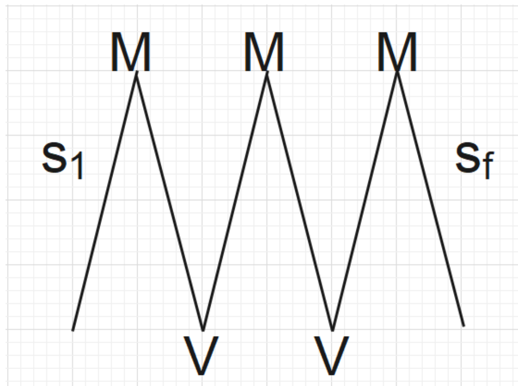

Figure 20: Example for Expression 18, 2 valleys and 3 mountains, hence $(2-3)\pi = -\pi$ and unravels completely.

between s_1 and s_f (Expression 18) (Figure 20).

$$(V - M)\pi = \beta \tag{18}$$

Through experimentation, it is possible to find a pattern between β values and complete unraveling (Table 3). Based on the results (Table 3), the

M value	V value	β value	Completely unraveled
4	1	3π	False
3	1	2π	False
3	2	π	True
3	3	0	True
2	3	$-\pi$	True
1	3	-2π	False
1	4	-3π	False

Table 3: Tabulation of β values and whether the design unraveled completely

structure completely unravels when $\beta = \pi, 0$, or $-\pi$ (Table3). This can be explained using a single crease. When $|\beta| > \pi$ there is only one pulling force (Figure 21; green arrow) acting on the crease, generating an equal and opposite normal force in accordance with Newton's third law (Figure 21; orange arrow). In this case, the structure can only unravel by curving a face, which is prohibited in rigid origami (Definition 3), hence the crease cannot be unraveled. This conclusion is based on observations where faces curved to allow unraveling.

Figure 21: Generation of a counteracting normal force

On the other hand when $|\beta| = \pi$ each pulling force unfolds less than π radians, producing no opposing force of equal magnitude, hence unravels.

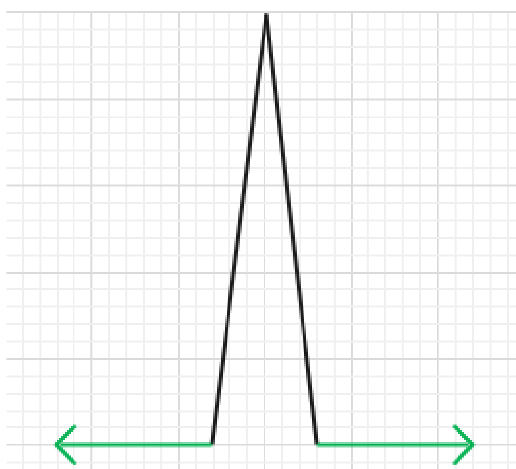

Figure 22: Simplified unfolding process when $\beta = |\pi|$

Therefore, Expression 19 is one of the criteria for unraveling multi-vertex designs. When both Expression 11 and 19 are true, multi-vertex designs unravel completely.

$$|V - M| < 2 \tag{19}$$

4.2 Force distribution

The second challenge is how multi-vertex origami distributes forces when unraveling. Observations show that some creases where the line of tension T does not intersect also unravel for some designs, like the Miura pattern (Figure 23) (Misseroni et al. 2024; Meloni et al. 2021). Explaining this obser-

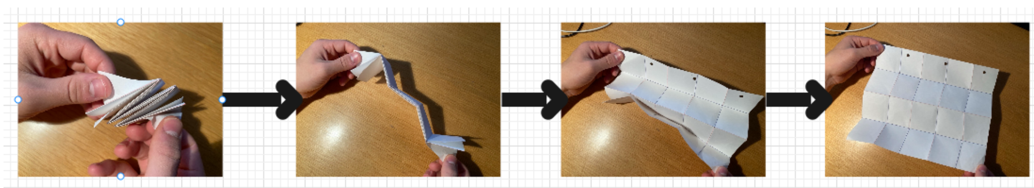

Figure 23: Unraveling of the Miura pattern

vation fully is challenging, however, the property, degree of freedom (DOF), helps understand and predict some features. DOF is "the number of independent parameters or values required to specify the *state* of an object" (Baker and Haynes 2024). In terms of origami, it implies the number of fold angles that must be known to predict the fold angle of all other creases, and DOF can be found using adjacency matrix (Yu, Guo, and Wang 2018). Based on the definition of DOF, it was hypothesized that an origami structure would completely unravel if the number of creases T intersecting in the completely unraveled state is greater or equal to the DOF of the structure. This would be true if creases were considered unraveled when $|\theta| < \pi$, as all fold angles must change when the number of creases intersecting T equals DOF, according to the definition. However, creases are only considered unraveled when $\theta = 0$, hence the situation is significantly more complex. This is supported by observations where the origami unravels completely or incompletely. It is thought to be predictable through the crease pattern force distribution, however, no pattern was discovered in this research. Part of the difficulty lies in the identification of complete and incompletely unraveling. Therefore, to explore this in further detail, one should either use a more rigid material, such as plastic, or take a more theoretical approach.

Because of this obstacle, the research question cannot be answered fully, but the criteria found throughout the essay allow for an evaluation algorithm to correctly evaluate all rigid flat foldable origami except multi-vertex designs where the line of tension (T) do not intersect all creases.

5 Unravelability Evaluation Algorithm

To address the research question, an evaluation algorithm was developed, represented as a flow chart (Figure 24) (inspired by Yu, Guo, and Wang (2018)), and is named Unravelability Evaluation Algorithm. It integrates all the methods developed in this essay into a logic chain, enabling the evaluation of whether an origami design will unravel or not, and whether it will unravel completely or incompletely. When the algorithm is given a crease pattern and the two points of pull (P_1, P_2), which forms the line of tension $(T = \overline{P_1P_2})$. A computational variable x ($x \in \{1, 2, ..., n\}$) cycles through integer values, and n represents the total number of creases. For computational simplicity, the following conventions are applied: $C_1 = C_{n+1}$ and $C_0 = C_n$. Additionally, $C_{1\to n}$ denotes the process of checking for all creases from C_1 to C_n. The algorithm's computational framework makes it easy to code a computer program, increasing the practicality of this Extended Essay's answer to the research question.

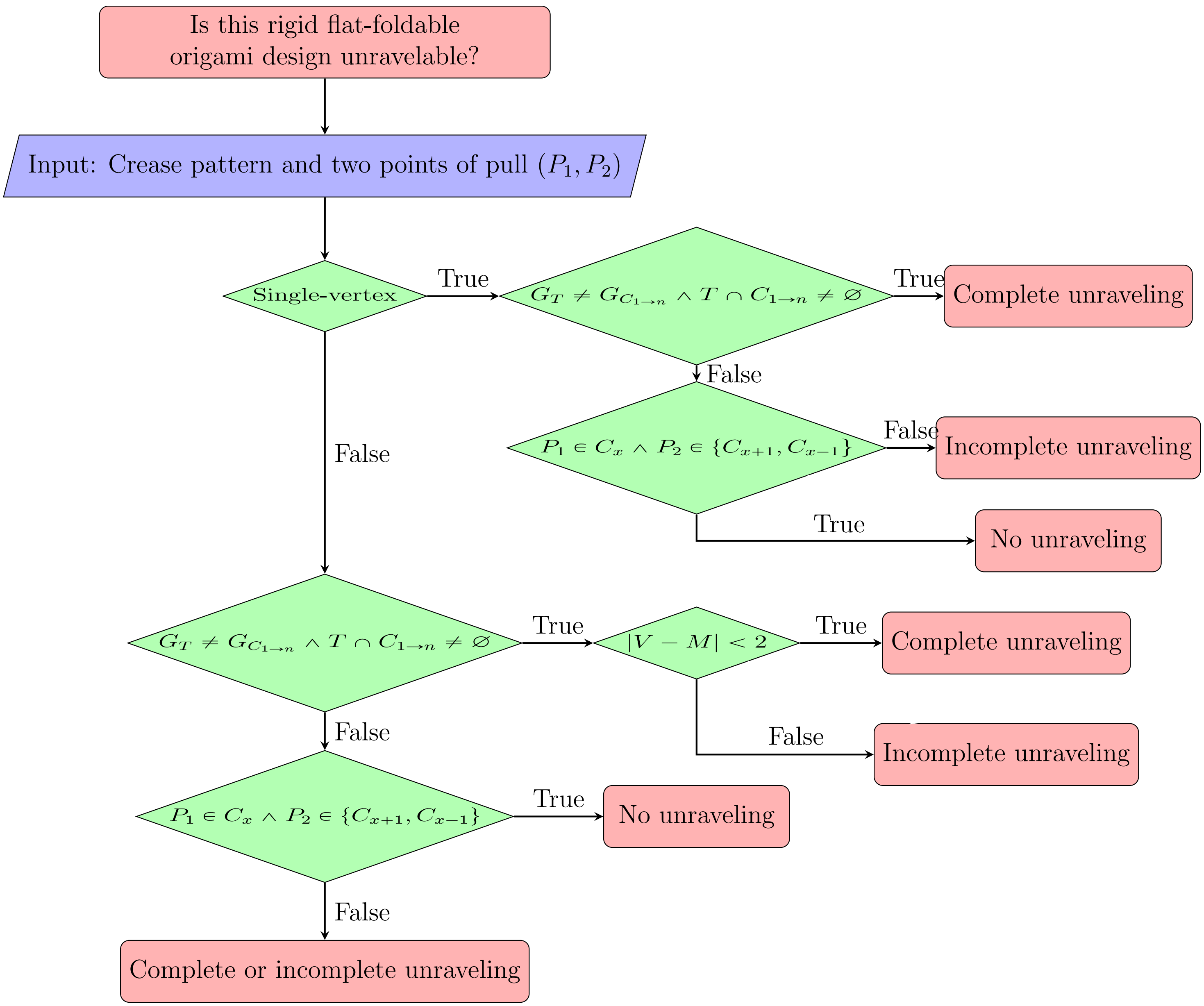

Figure 24: Flow chart of Unravelability Evaluation Algorithm, inspired by Yu, Guo, and Wang (2018)

6 Conclusion

In this essay, the research question "How to mathematically evaluate whether a rigid flat-foldable origami design will unravel or not, and whether it will unravel completely or incompletely when pulled from two points?" has been explored. To answer this question, definitions and theoretical frameworks were established, and origami structures of varying complexities were investigated. The resulting Unravelability Evaluation Algorithm (Figure 24) was developed cumulatively through theorems developed in this essay, providing accurate answers for single-vertex designs and multi-vertex designs where Expression 11 is true. Thereby reducing the need for costly and time-consuming physical tests, providing a robust tool for applying origami mechanics. Despite the algorithm's strengths allowing the Extended Essay to answer the research question to a high degree, the algorithm has limitations. Specifically, it cannot predict unraveling force distributions in complex multi-vertex designs, restricting the essay's ability to answer the research question. This highlights the need for future research to address this gap and extend the algorithm's capabilities. Additionally, expanding the research to include non-flat foldable origami would broaden the algorithm's applicability and enhance its relevance in the field. By addressing these limitations and extending the scope, the potential of origami mechanics can be fully realized opening doors to advancements in a wide range of fields such as nano-robotics, material science, and aerospace.

References

Baker, D. W. and W. Haynes (Aug. 2024). "Engineering Statics: Open and Interactive". In: Engineering Statics. Chap. 5.1 Degree of Freedom. URL: https://engineeringstatics.org/Chapter_05-degree-of-freedom.html.

Ben-Ari, M. (2022). "The Axioms of Origami". In: *Mathematical Surprises*. Cham: Springer International Publishing, pp. 113–130.

Deleo, A. A. et al. (2020). "Origami-based deployable structures made of carbon fiber reinforced polymer composites". In: *Composites Science and Technology* 191, p. 108060. DOI: 10.1016/j.compscitech.2020.108060.

Dureisseix, D. (Mar. 2012). "An Overview of Mechanisms and Patterns with Origami". In: *International Journal of Space Structures* 27, pp. 1–14. DOI: 10.1260/0266-3511.27.1.1.

Eppstein, D. (2018). "Realization and Connectivity of the Graphs of Origami Flat Foldings". In: *Graph Drawing and Network Visualization*. Ed. by T. Biedl and A. Kerren. Cham: Springer International Publishing, pp. 541–554.

Flaum, E. and M. Prakash (2024). "Curved crease origami and topological singularities enable hyperextensibility of L. olor". In: *Science* 384.6700, eadk5511. DOI: 10.1126/science.adk5511.

Hull, T. C. (2021). *Origametry: Mathematical Methods in Paper Folding*. Cambridge University Press.

Lang, R. J. (1996). "A computational algorithm for origami design". In: *Proceedings of the Twelfth Annual Symposium on Computational Geometry*. SCG '96. Philadelphia, Pennsylvania, USA: Association for Computing Machinery, pp. 98–105. DOI: 10.1145/237218.237249.

— (2011). *Origami Design Secrets: Mathematical Methods for an Ancient Art, Second Edition*. Taylor & Francis.

Meloni, M. et al. (2021). "Engineering Origami: A Comprehensive Review of Recent Applications, Design Methods, and Tools". In: *Advanced Science* 8.13, p. 2000636. DOI: 10.1002/advs.202000636.

Misseroni, D. et al. (2024). "Origami engineering". In: *Nature Reviews Methods Primers* 4.1, p. 40. DOI: 10.1038/s43586-024-00313-7.

Mitani, J. (2012). *ORIPA: Origami Pattern Eidtor*. [online]. Accessed: 02.09.2024. URL: https://mitani.cs.tsukuba.ac.jp/oripa/.

Tachi, T. (Aug. 2009). "Simulation of Rigid Origami". In: *Origami 4: Fourth International Meeting of Origami Science, Mathematics, and Education* 4. DOI: 10.1201/b10653-20.

Talagrand, M. (16 May 2024). *Åpen forelesning med årets abelprisvinner*. [Lecture]. 16 May. University of Stavanger.

Yu, H., Z. Guo, and J. Wang (2018). "A method of calculating the degree of freedom of foldable plate rigid origami with adjacency matrix". In: *Advances in Mechanical Engineering* 10.6, p. 1687814018779696. DOI: 10.1177/1687814018779696.